

# Epsilon\*: Privacy Metric for Machine Learning Models

Diana M. Negoescu<sup>1</sup>, Humberto Gonzalez<sup>1</sup>, Saad Eddin Al Orjany<sup>1</sup>, Jilei Yang<sup>1</sup>,  
Yuliia Lut<sup>1</sup>, Rahul Tandra<sup>1</sup>, Xiaowen Zhang<sup>1</sup>, Xinyi Zheng<sup>1</sup>, Zach Douglas<sup>1</sup>,  
Vidita Nolkha<sup>1</sup>, Parvez Ahammad<sup>1</sup>, and Gennady Samorodnitsky<sup>1, 2</sup>

<sup>1</sup>LinkedIn Corporation

<sup>2</sup>Cornell University

July 24, 2023

## Abstract

We introduce Epsilon\*, a new privacy metric for measuring the privacy risk of a single model instance prior to, during, or after deployment of privacy mitigation strategies. The metric does not require access to the training data sampling or model training algorithm. Epsilon\* is a function of true positive and false positive rates in a hypothesis test used by an adversary in a membership inference attack. We distinguish between quantifying the privacy loss of a trained model instance and quantifying the privacy loss of the training mechanism which produces this model instance. Existing approaches in the privacy auditing literature provide lower bounds for the latter, while our metric provides a lower bound for the former by relying on an  $(\epsilon, \delta)$ -type of quantification of the privacy of the trained model instance. We establish a relationship between these lower bounds and show how to implement Epsilon\* to avoid numerical and noise amplification instability. We further show in experiments on benchmark public data sets that Epsilon\* is sensitive to privacy risk mitigation by training with differential privacy (DP), where the value of Epsilon\* is reduced by up to 800% compared to the Epsilon\* values of non-DP trained baseline models. This metric allows privacy auditors to be independent of model owners, and enables all decision-makers to visualize the privacy-utility landscape to make informed decisions regarding the trade-offs between model privacy and utility.

## 1 Introduction

Many machine learning (ML) models are trained using either private customer data (age, gender, but also quasi-identifiers such as geographical location), or using third-party information. In order to offer data-driven privacy protections in the context of increasing demand for privacy protection, model owners need metrics that help quantify the privacy risk in their artificial intelligence models, in addition to privacy risk mitigation strategies which reduce the risk once the metrics identify it as high.

In this paper, we start with an  $(\epsilon, \delta)$ -type of quantification of the privacy of a trained model instance and derive a lower bound for the  $\epsilon$  in this quantification inspired by the hypothesis test characterization of differential privacy (DP) in [Kairouz et al.(2015)]. We use this lower bound, which we refer to as Epsilon\*, as a privacy metric in and of itself, as it has several desirable properties. Specifically, Epsilon\*:

- does not interfere with the training pipeline, i.e., it does not require model re-training or re-sampling of the training set. While obtaining statistically valid lower bounds on the DP parameter  $\epsilon$  requires model re-training, or, at a minimum, re-sampling the training set to introduce “canaries” [Steinke et al.(2023)], obtaining a valid lower bound on model

privacy does not require either. This is important, as privacy analyzers might not have access to the input or training pipeline of models, and deployed models in the industry are often very large and require many hours or days to train, rendering their re-training prohibitive.

- enables model owners to prioritize which training pipelines to be mitigated with DP. Epsilon\* can be computed on any ML model instance, including on model instances from training mechanisms where DP hasn't been deployed yet. DP is the gold standard privacy mitigation strategy, but comes with well-documented computational and utility drawbacks, e.g. [Denison et al.(2022), Ponomareva et al.(2023)]. We make a distinction between *mitigating* and *measuring* privacy risk of models: in particular, training with DP is a mitigation strategy, while Epsilon\* provides a measurement of privacy loss on a given model instance. Even though training with DP ensures model-level privacy and its  $\epsilon$  parameter in DP is a measurement of worst-case privacy loss, it is not trivial for auditors agnostic of the training mechanism to determine whether or not DP was used in training and if so, with what  $\epsilon$  parameter, as recent advances in the area of auditing DP [Steinke et al.(2023), Nasr et al.(2023), Zanella-Béguelin et al.(2022)] assume knowledge of whether or not DP was used, in addition to access to the training pipeline for re-sampling or model re-training.
- can quantify privacy at all stages of model development and deployment, including when privacy mitigation strategies do not involve DP. For instance, model owners may investigate the effects on privacy when iterating through model development stages of feature addition or removal, or of training the model for more or fewer epochs.

In this paper, we introduce Epsilon\* and show how to derive it from the true positive (TPR) and false positive rates (FPR) of a hypothesis test of a simulated membership inference attack (MIA) on population data (MIA-PD) [Shokri et al.(2017), Yeom et al.(2018)], where an attacker attempts to predict whether a given data point was used for model training based on the training and non-training loss distributions from a given model instance. We note that the hypothesis test formulation is not restrictive to this particular attack, and in fact Epsilon\* could be derived from any other attacks that can be formulated as hypothesis tests on neighboring data sets, such as attribute inference attacks (AIAs) [Yeom et al.(2018)]. We chose MIA-PD as it is a canonical privacy attack, requiring minimum (black box) model access by the attacker, and is the foundation of stronger attacks such as AIAs [Carlini et al.(2022)].

We map challenges in the implementation of Epsilon\*, coming from the fact that often the most impactful TPR and FPR realizations are those close to 0 and 1, where sampling noise and numerical floating point errors are prone to occur. We show that we can avoid these pitfalls by working with a parametric distributions fitted to a transformation of the loss data, where an analytical formulation to Epsilon\* is also available.

Our main contributions are two-fold: on the theoretical side, we prove that a statistical relationship between Epsilon\* and a lower bound on the privacy loss parameter  $\epsilon$  of the training mechanism exists. On the empirical side, we compute Epsilon\* for a range of model instances trained on public data sets (UCI Adult, Purchase-100), with varying privacy mitigation strategies (without DP and with DP for various DP  $\epsilon$  values), and a range of model hyper-parameter configurations. Our experiments show that Epsilon\* is sensitive to privacy mitigation with DP, and in particular its value was below that of the  $\epsilon$  used when training with DP in almost all model instances<sup>1</sup>.

---

<sup>1</sup>Our experiments showed that Epsilon\* values were less than the  $\epsilon$  used when training with DP when the latter was at least 1. In simulations shown in Appendix B, we observed that when training and non-training loss distribution were identical, i.e., Epsilon\* should be 0, small sample sizes could lead to over-estimation (values higher than 0). This effect was mitigated by parametrizing loss distributions (Section 3.2) and increasing sample size.

## 2 Background and Related Work

The standard definition of differential privacy of a randomized mechanism  $M$  taking as an argument a database  $D$  and outputting a value in some set  $\mathcal{Z}$  [Dwork et al.(2006)], is

$$Pr[M(D_0) \in R] \leq e^\epsilon Pr[M(D_1) \in R] + \delta \quad (1)$$

for all pairs of neighboring databases  $D_0$  and  $D_1$  that differ in the record of a single individual and for every (measurable) subset  $R \subset \mathcal{Z}$ . A mechanism with this property is called  $(\epsilon, \delta)$ -DP.

A powerful hypothesis test characterization of DP was introduced by [Kairouz et al.(2015)], and later expanded by [Dong et al.(2022)] in defining Gaussian differential privacy. Here, one views a set  $R$  as the rejection (critical) region of the statistical test

$$\begin{aligned} H_0 &: \text{the mechanism was run on the database } D_0, \\ H_1 &: \text{the mechanism was run on the database } D_1 \end{aligned}$$

for some fixed neighboring databases  $D_0$  and  $D_1$ .

**Theorem 1** ([Kairouz et al.(2015)]). *A mechanism  $M$  is  $(\epsilon, \delta)$  - differentially private if and only if the following conditions are satisfied for all pairs of neighboring databases  $D_0$  and  $D_1$ , and all rejection regions  $R$ :*

$$\begin{aligned} Pr[M(D_0) \in R] + e^\epsilon Pr[M(D_1) \in \bar{R}] &\geq 1 - \delta \\ Pr[M(D_1) \in \bar{R}] + e^\epsilon Pr[M(D_0) \in R] &\geq 1 - \delta, \end{aligned}$$

where  $\bar{R}$ , the acceptance region, is the complement of  $R$ . Here,  $Pr[M(D_0) \in R]$  is the false negative rate (FNR) (Type I error) and  $Pr[M(D_1) \in \bar{R}]$  is the false positive rate (FPR)(Type II error) for the hypothesis test above.

MIAs naturally define a hypothesis test for whether a target entry belongs to the training set or not [Shokri et al.(2017), Yeom et al.(2018), Carlini et al.(2022)]. However, it is important to realize that the test is based on the loss of the trained model on a query point, not the change in the model weights resulting from adding or removing the query point from the training data set. Therefore, the hypothesis testing setup and the corresponding notions of FNR and FPR have to be modified. In MIA-PD, attackers usually choose a threshold  $\tau$ , and classify any point whose model loss is above  $\tau$  as non-training: the test statistic is then the model loss and the corresponding rejection region  $R$  for this hypothesis test is the interval  $[\tau, \infty)$  [Yeom et al.(2018), Salem et al.(2018), Ye et al.(2022)].

Most advances in the growing area of auditing differential privacy have also been built upon hypothesis testing framework inspired by Theorem 1: [Ding et al.(2018), Bichsel et al.(2018), Jagielski et al.(2020), Nasr et al.(2021), Tramer et al.(2022), Zanella-Béguelin et al.(2022)]. Indeed, estimating a pair of (FNR, FPR) in the hypothesis test of Theorem 1 provides a lower bound on the  $\epsilon$  parameter of the mechanism  $M$ , which can be used to detect mistakes in the implementation of the mechanisms leading to higher privacy loss values than intended. However, if  $M$  is an ML mechanism, then multiple runs of re-sampling and re-training the models are necessary for the statistical estimation of the FNRs and FPRs, ranging from the order of thousands when Clopper-Pearson methods are used in statistical estimation [Nasr et al.(2021), Tramer et al.(2022)] to about 500 when Bayesian methods are employed [Zanella-Béguelin et al.(2022)].

Several suggestions on evaluating the privacy of training mechanisms while reducing the number of times models need to be re-trained in order to estimate the lower bound on the  $\epsilon$  have been made recently [Lu et al.(2022), Steinke et al.(2023)], in particular in the area of federated learning [Andrew et al.(2023), Maddock et al.(2022), Nasr et al.(2023)]. Several of these methods now only require one [Steinke et al.(2023)] or two models [Nasr et al.(2023)] to

be re-trained, but all of them still require access to the sampling of the data sets used for model training for introducing canaries [Steinke et al.(2023), Maddock et al.(2022)], and/or visibility into model updates during training [Nasr et al.(2023)]. As we pointed out above, measuring privacy in the ML context is tricky, and not all methods in the literature address the same type of resilience against an attack.

In this paper, we propose an estimator for the lower bound on the privacy risk against MIAs of a single model instance rather than on the privacy risk of the training mechanism that generates the model instances. This enables privacy auditors to be independent of model owners when evaluating the privacy loss of a model, paving the way for transparent and easy to implement measurements of privacy risk. We advocate for using this estimator as a privacy metric in and of itself, as it shows sensitivity to privacy mitigation strategies such as DP when evaluated on deep neural net model instances trained on public data sets.

### 3 Methods

The definition of differential privacy in (1) needs to be adapted for ML applications where we are interested in measuring the resilience of a trained ML model instance against an adversary performing a MIA.

Let  $\mathcal{X} \times \mathcal{Y}$  be the set of all possible observations  $(x, y)$  a ML training mechanism  $M$  may use for training, testing and/or validation, where  $x$  is usually a feature vector in  $\mathbb{R}^d$  and  $y$  is the label. Let  $\mathcal{P}$  be a distribution over  $\mathcal{X} \times \mathcal{Y}$ . The training mechanism takes as input a training data set  $D = \{(x_1, y_1), \dots, (x_n, y_n)\} \in (\mathcal{X} \times \mathcal{Y})^n$  sampled according to  $\mathcal{P}$  and outputs a trained model with weights  $\theta = M(D) \in \Theta$ , where  $\Theta$  is the space of all possible weights, i.e.,  $\theta$  is an observation of a (usually) random training mechanism  $M$  applied to data set  $D$ . The prediction of the model at observation  $x$  is then  $f_\theta(x)$ : for example, in binary classification models,  $f_\theta(x) \in \mathcal{Y} = [0, 1]$  is typically the probability of observing label  $y = 1$ , where we can think of  $y$  as taking values 0 or 1 in  $\mathcal{Y}$ . The MIA adversary formulates the hypothesis test:

$$\begin{aligned} H_0 &: \text{The training data set does not contain point } (x, y) \in \mathcal{X} \times \mathcal{Y}, \\ H_1 &: (x, y) \text{ belongs to the training data set.} \end{aligned}$$

The adversary has black box access to the trained model and makes a decision based on evaluating  $f_\theta(x)$  and comparing it with  $y$ . Therefore, the adversary utilizes as a rejection region a subset  $R \subset \mathcal{Y} \times \mathcal{Y}$  and rejects  $H_0$  (i.e. decides that the query point  $(x, y)$  was, in fact, used for training) if  $(f_\theta(x), y) \in R$ . The rejection region may be tailored to the trained model, and so it may be a function of the weights  $\theta$ :

$$R = R(\theta) = R(M(D)).$$

Our quantification of resilience of the trained model is given below. It is inspired by the  $(\epsilon, \delta)$ -parameterization of differential privacy in (1).

**Definition 1.** A trained model instance parameterized by  $\theta$ , and obtained from using a training mechanism on data set  $D = \{(x_i, y_i), i = 1, \dots, n\} \in (\mathcal{X} \times \mathcal{Y})^n$ , is  $(\epsilon, \delta)$ -private if for any (measurable) set  $R \subset \mathcal{Y} \times \mathcal{Y}$

$$\mathbb{P}_{(X,Y) \sim \bar{D}} [(f_\theta(X), Y) \in R] \leq e^\epsilon \mathbb{P}_{(X,Y) \sim D} [(f_\theta(X), Y) \in R] + \delta, \quad (2)$$

$$\mathbb{P}_{(X,Y) \sim D} [(f_\theta(X), Y) \in R] \leq e^\epsilon \mathbb{P}_{(X,Y) \sim \bar{D}} [(f_\theta(X), Y) \in R] + \delta, \quad (3)$$

where  $\bar{D} = (\mathcal{X} \times \mathcal{Y})^n \setminus D$  is the data not used for training,  $(X, Y) \sim \bar{D}$  refers to sampling from the conditional distribution  $\mathcal{P}$  given  $\{(X, Y) \notin D\}$ ,  $\mathbb{P}_{(X,Y) \sim D} [(f_\theta(X), Y) \in R] = \frac{1}{n} \sum_{i=1}^n \mathbf{1}((f_\theta(x_i), y_i) \in R)$ , and  $f_\theta(x)$  is the prediction of the trained model  $\theta$  with input  $x$ .

Notice that in our Definition 1, the randomness comes from sampling either from the training data set  $D$ , or from the non-training data  $\bar{D}$ , in contrast to the established DP definition (1), where the randomness is infused by the training mechanism  $M$ . On the other hand,  $\theta$  and  $D$  in Definition 1 are fixed (not random), as they are simply the model instance and data set observed by the auditor.

We provide the following analog of Theorem 1 in our model-level privacy quantification (Definition 1):

**Theorem 2.** *A trained model instance parameterized by  $\theta$ , and obtained from using a training mechanism  $M$  on data set  $D = \{(x_i, y_i), i = 1, \dots, n\}$ , is  $(\epsilon, \delta)$ -private if and only if for all rejection regions  $R$ :*

$$\mathbb{P}_{(X,Y) \sim \bar{D}} [(f_\theta(X), Y) \in R] + e^\epsilon \mathbb{P}_{(X,Y) \sim D} [(f_\theta(X), Y) \in \bar{R}] \leq e^\epsilon + \delta \quad (4)$$

$$\mathbb{P}_{(X,Y) \sim D} [(f_\theta(X), Y) \in \bar{R}] + e^\epsilon \mathbb{P}_{(X,Y) \sim \bar{D}} [(f_\theta(X), Y) \in R] \geq 1 - \delta \quad (5)$$

$$\mathbb{P}_{(X,Y) \sim \bar{D}} [(f_\theta(X), Y) \in R] + e^\epsilon \mathbb{P}_{(X,Y) \sim D} [(f_\theta(X), Y) \in \bar{R}] \geq 1 - \delta \quad (6)$$

$$\mathbb{P}_{(X,Y) \sim D} [(f_\theta(X), Y) \in \bar{R}] + e^\epsilon \mathbb{P}_{(X,Y) \sim \bar{D}} [(f_\theta(X), Y) \in R] \leq e^\epsilon + \delta \quad (7)$$

where  $\bar{D}$  is the part of the data not used for training, and  $f_\theta(x)$  is the prediction of the trained model  $\theta$  with input  $x$ .

The proof of Theorem 2 follows easily from Definition 1, just like Theorem 1 follows easily from the DP definition in Equation (1): (4) and (5) are directly from (2) and (3) respectively, and (6) and (7) follow from (2) and (3) by replacing  $R$  with  $\bar{R}$ .

To understand how we choose  $R$  in Definition 1 and Theorem 2, let  $l(f_\theta(x), y)$  be a loss function<sup>2</sup> of the model with weights  $\theta$  under input  $(x, y)$ . The output  $\theta$  of the trained model generates a population (non-training) loss distribution resulting from sampling a point from  $\bar{D}$  and evaluating the loss of the trained model on that point. Similarly, the output  $\theta$  of the trained model generates a training data loss distribution that results from sampling at random a point from the training data set and evaluating the loss of the trained model on that point. The losses on the training data set tend to be smaller than the losses on non-training (population) data [Jayaraman et al.(2020)], therefore the adversary may select a threshold  $\tau$  and reject  $H_0$  (i.e. conclude that the query point  $(x, y)$  was used for training) if the loss  $l(f_\theta(x), y) \leq \tau$ . This corresponds to setting

$$R = R(\theta) = \{(y_1, y_2) \in \mathcal{Y} \times \mathcal{Y} : l(y_1, y_2) \leq \tau\} \quad (8)$$

above.

We parametrize  $\tau$  as  $\tau = q_t(\theta)$ , a quantile of the non-training loss distribution with value  $\tau$ . Therefore,

$$\mathbb{P}_{(X,Y) \sim \bar{D}} [(f_\theta(X), Y) \in R] = \mathbb{P}_{(X,Y) \sim \bar{D}} [l(f_\theta(X), Y) \leq q_t(\theta)] = t, \quad (9)$$

this gives us the false positive rate (FPR)  $t$  in the MIA hypothesis test. We denote by  $\eta_t$  the corresponding false negative rate (FNR):

$$\mathbb{P}_{(X,Y) \sim D} [(f_\theta(X), Y) \in \bar{R}] = \mathbb{P}_{(X,Y) \sim D} [l(f_\theta(X), Y) > q_t(\theta)] = \eta_t, \quad (10)$$

We can obtain a valid lower bound on  $\epsilon$  in Definition 1 by utilizing Theorem 2, and exploiting the intuition that any  $\epsilon$  value that is smaller than the minimum value satisfying Eq. (4 - 7) is a counter-example to the model being  $(\epsilon, \delta)$ -private as in Definition 1. Therefore, a valid lower bound on the resilience of that model instance can be obtained by solving the following linear

<sup>2</sup>We use  $l(f_\theta(x), y) = (1 - 2y)(\log(f_\theta(x)) - \log(1 - f_\theta(x)))$  for binary classification models and  $l(f_\theta(x), y) = -\sum_j (\log(f_\theta(x)_j) - \log(1 - f_\theta(x)_j)) \mathbf{1}_{\{y_j=1\}}$  for multi-class classification models, where  $j$  is an index over the classes.

program, where the constraints come from Eq. (4 - 7) with the FPR and TPR notation of (9) and (10):

$$\begin{aligned}
& \text{minimize} && \epsilon \\
& \text{subject to} && t + e^\epsilon \eta_t \leq e^\epsilon + \delta \\
& && \eta_t + e^\epsilon t \geq 1 - \delta \\
& && t + e^\epsilon \eta_t \geq 1 - \delta \\
& && \eta_t + e^\epsilon t \leq e^\epsilon + \delta.
\end{aligned}$$

To improve this lower bound (i.e., find a higher one), we select multiple quantiles  $t_1, \dots, t_k$  in (9) and constructing  $k$  different rejection regions corresponding to these levels,  $R_1(\theta), \dots, R_k(\theta)$ . By definition (9), the false positive rate corresponding to the rejection region  $R_i(\theta)$  is exactly  $t_i$ ,  $i = 1, \dots, k$ , and we let  $\eta_i$  be the false negative rate corresponding to the rejection region  $R_i(\theta)$ . Then, each line in the linear program above will describe  $k$  constraints corresponding to the  $k$  rejection regions, and its solution,  $\epsilon^*$  in the following definition, is a valid lower bound for  $\epsilon$  in Definition 1 by Theorem 2.

**Definition 2** (Epsilon\*). *Let  $\delta$  be a small non-negative real number, and  $\{(t_i, \eta_i)\}_{i=1, \dots, k}$  be the false positive and false negative rates, respectively, corresponding to  $k$  rejection regions  $\{R_i(\theta)\}_{i=1, \dots, k}$  of the form (8), where each  $t_i$  and  $\eta_i$  is described by Equations (9) and (10) respectively. We call the following quantity Epsilon\*:*

$$\epsilon^* = \log \left[ \max_{i=1, \dots, k} \max \left( \frac{1 - \delta - \eta_i}{t_i}, \frac{1 - \delta - t_i}{\eta_i}, \frac{\eta_i - \delta}{1 - t_i}, \frac{t_i - \delta}{1 - \eta_i} \right) \right] \quad (11)$$

The  $\delta$  in Definition 2 should be chosen as the same  $\delta$  in Definition 1, as  $\epsilon^*$  is a lower bound for  $\epsilon$  in Definition 1 given the same  $\delta$ . Just as in the original DP definition from [Dwork et al.(2006)], the  $\delta$  in our Definition 1 controls the amount of relaxation in how much the probabilities can differ. The general recommendation in the DP literature is to set  $\delta \ll 1/n$ , where  $n$  is the number of records in the training set [Ponomareva et al.(2023)], as this implies that each record in the training set has a worst case probability  $\delta$  of being identified, and if  $\delta \ll 1/n$ , then the expected number of successfully identified records is less than 1. We recommend setting the  $\delta$  in Epsilon\* (and Definition 1) by the same guidelines.

The best lower bound of this type is obtained when we choose the quantiles  $(t_i)$  densely, i.e. let  $k \rightarrow \infty$ . This observations turns out to be very useful in the parametric Epsilon\* described in Section 3.2 and Appendix B.

### 3.1 Epsilon\* vs lower bounds for the privacy loss of the training mechanism

One can, in fact, define a version of Epsilon\* for the training mechanism itself, and obtain a statistically valid lower bound, say  $\bar{\epsilon}$ , on the  $(\epsilon, \delta)$ -privacy quantification of the training mechanism. Recall that, generally,  $\theta$  in Definition 1 is an observation from a random variable – obtained by applying random training mechanism  $M$  to data set  $D$ . Correspondingly, we view the lower bound  $\epsilon^*$  corresponding to a model instance as an observation from a random variable (a function of the training mechanism). Under an appropriate setup, there is a connection between the mechanism-level  $\bar{\epsilon}$  and the model-level random  $\epsilon^*$ <sup>3</sup>. We now provide the setup and the connection between these quantities .

Suppose that instead of measuring the resilience of a trained model we now wish to measure the resilience of the training mechanism. Consider the probabilities on the left sides of the

<sup>3</sup>We note that Epsilon\* can also be computed for model instances from deterministic training algorithms such as boosted decision trees, since it does not require any prior knowledge of the training algorithm beyond the given model instance. In such deterministic cases, however, we cannot talk about lower bounds for differential privacy mechanisms, as those mechanisms would require infusing randomness.

inequalities in Definition 1 for any choice of (measurable) rejection regions  $R_\theta$  of the form (8), with additional averaging over choices of the training sets and randomness of the training mechanism:

$$E_{D,\theta} \left[ \mathbb{P}_{(X,Y) \sim \bar{D}} [(f_\theta(X), Y) \in R_\theta] \right] \leq e^\epsilon E_{D,\theta} \left[ \mathbb{P}_{(X,Y) \sim D} [(f_\theta(X), Y) \in R_\theta] \right] + \delta, \quad (12)$$

$$E_{D,\theta} \left[ \mathbb{P}_{(X,Y) \sim D} [(f_\theta(X), Y) \in R_\theta] \right] \leq e^\epsilon E_{D,\theta} \left[ \mathbb{P}_{(X,Y) \sim \bar{D}} [(f_\theta(X), Y) \in R_\theta] \right] + \delta, \quad (13)$$

where  $E_{D,\theta}$  is the expectation taken with respect to the randomness producing training set  $D \sim \mathcal{P}^n$  and the randomness infused by the training mechanism, where  $\theta = M(D)$ ,  $(X, Y) \sim \bar{D}$  refers to sampling from the conditional distribution  $\mathcal{P}$  given  $\{(X, Y) \notin D\}$ , and  $\mathbb{P}_{(X,Y) \sim D} [(f_\theta(X), Y) \in R] = \frac{1}{n} \sum_{i=1}^n \mathbf{1}((f_\theta(x_i), y_i) \in R)$  as in Definition 1. Furthermore, note that  $\bar{D}$ , the data not used for training, depends on the choice of training set  $D$  which is now random, and therefore itself becomes random.

The following result states that differential privacy implies (12) and (13), and therefore these two equations can be used to derive a lower bound on the privacy loss of DP, which we call  $\bar{\epsilon}$ , similar to how we used our Definition 1 to derive Epsilon\*.

**Theorem 3.** *Let  $M$  be an  $(\epsilon, \delta)$ -differentially private training mechanism that generates model instances parameterized by  $\theta$  given data sets  $D$ , and let  $\bar{D}$  be the population of the data excluding  $D$ .*

*Then, any  $\bar{\epsilon}$  that satisfies (12) and (13) for any choice of rejection region  $R_\theta$  of the form (8), is a lower bound for the  $\epsilon$  parameter of  $M$  for the same value of  $\delta$ .*

The proof of Theorem 3 can be found in Appendix A.

We now find an expression for  $\bar{\epsilon}$  along the same lines as Theorem 1 (recently also used by [Zanella-Béguelin et al.(2022)]). Suppose we choose a rejection region  $R_\theta$  of the form (8) with quantile  $q_t(\theta)$  still chosen according to (9). Note that now the population loss distribution may change from instance to instance, so the critical set  $R_\theta$  will change even if we keep the level  $0 < t < 1$  in (9) constant (not  $\theta$  dependent). Fixing a  $t$  independently of  $\theta$ , recall that by (9),  $\mathbb{P}_{(X,Y) \sim \bar{D}} [(f_\theta(X), Y) \in R] = \mathbb{P}_{(X,Y) \sim \bar{D}} [l(f_\theta(X), Y) \leq q_t(\theta)] = t$ , for any trained weights  $\theta$ . The false positive rate for the mechanism-level hypothesis test is then

$$FPR = E_{D,\theta} \left[ \mathbb{P}_{(X,Y) \sim \bar{D}} [(f_\theta(X), Y) \in R_\theta] \right] = t.$$

Note that the corresponding mechanism-level false negative rate, FNR, is

$$\eta_t = FNR = E_{D,\theta} \left[ \frac{1}{n} \sum_{i=1}^n \mathbf{1}(l(f_\theta(X_i), Y_i) > q_t(\theta)) \right] := E_{D,\theta} (\eta_t(\theta)), \quad (14)$$

where we view  $\eta_t(\theta)$  as the FNR corresponding to a fixed model  $\theta$ ,  $l(f_\theta(X_i), Y_i)$  is the loss of the model  $\theta$  at point  $(X_i, Y_i)$ , and  $D = \{(X_i, Y_i)_{i=1,\dots,n}\}$  is a sampled training set.

A lower bound on the privacy loss of a differentially private mechanism is then

$$\bar{\epsilon} = \log \left[ \max_{i=1,\dots,k} \max \left( \frac{1 - \delta - \eta_{t_i}}{t_i}, \frac{1 - \delta - t_i}{\eta_{t_i}}, \frac{\eta_{t_i} - \delta}{1 - t_i}, \frac{t_i - \delta}{1 - \eta_{t_i}} \right) \right] \quad (15)$$

with  $\eta_{t_i}$  given by (14).

On the other hand, Epsilon\* for a given model  $\theta$  is random, and given by

$$\epsilon^* = \epsilon^*(\theta) = \log \left[ \max_{i=1,\dots,k} \max \left( \frac{1 - \delta - \eta_{t_i}(\theta)}{t_i}, \frac{1 - \delta - t_i}{\eta_{t_i}(\theta)}, \frac{\eta_{t_i}(\theta) - \delta}{1 - t_i}, \frac{t_i - \delta}{1 - \eta_{t_i}(\theta)} \right) \right]. \quad (16)$$

With this setup, we have the following result connecting this random  $\epsilon^*$  with the lower bound  $\bar{\epsilon}$  on the  $(\epsilon, \delta)$ -differential privacy of a training mechanism.

**Theorem 4.** Let  $\bar{\epsilon}$  be the mechanism-level lower bound on privacy loss as in (15), and let  $\epsilon^* = \epsilon^*(\theta)$  be the (random) individual model-level lower bound on privacy loss as in (16). Then

$$\bar{\epsilon} \leq \log \left[ E_{\theta} \left( e^{\epsilon^*} \right) \right] \quad (17)$$

The proof of Theorem 4 can be found in Appendix A.

### 3.2 Parametric Epsilon\*

We show in Appendix B that estimating FNRs and FPRs from the empirical loss distributions can lead to unstable implementations of Epsilon\* due to the fact that most relevant FNR and FPR values are usually those very close to 0 and 1, where noise is also likely to become amplified by the maximization in (11). We avoid this instability by fitting parametric Gaussian models to the training and non-training (population) loss distributions, where we first normalize the losses to  $[0,1]$ , and then apply a logit transformation similar to the one used by [Carlini et al.(2022)] (Appendix B). Evaluating the cumulative distribution functions (CDFs) of the fitted parametric distributions to loss data instead of evaluating the empirical CDFs of the training and non-training loss data results in an improved accuracy and sensitivity of Epsilon\*, as we show in Appendix B.

Let  $F^{pop}$  and  $F^{tr}$  be the cumulative distribution functions for the fitted parametric distributions to the population and training loss data respectively. Recall that for  $0 < t < 1$ , we select  $q_t = q_t(\theta)$  to be the  $t$ -quantile of  $F^{pop}$  in (9), so that  $q_t = (F^{pop})^{-1}(t)$ . The FPR is  $t$  by equation (9), and the corresponding FNR is

$$\eta_t = 1 - F^{tr}(q_t). \quad (18)$$

If  $F^{pop}$  and  $F^{tr}$  are parametric distributions, we can obtain a higher lower bound than in (11) by computing Epsilon\* as

$$\epsilon^* = \log \left[ \sup_{0 < t < 1} \max \left( \frac{1 - \delta - \eta_t}{t}, \frac{1 - \delta - t}{\eta_t}, \frac{\eta_t - \delta}{1 - t}, \frac{t - \delta}{1 - \eta_t} \right) \right] \quad (19)$$

$$= \log \left[ \max \left( \sup_{0 < t < 1} \frac{1 - \delta - \eta_t}{t}, \sup_{0 < t < 1} \frac{1 - \delta - t}{\eta_t}, \sup_{0 < t < 1} \frac{\eta_t - \delta}{1 - t}, \sup_{0 < t < 1} \frac{t - \delta}{1 - \eta_t} \right) \right] \quad (20)$$

$$=: \log [\max(m_1, m_2, m_3, m_4)] \quad (21)$$

The values  $m_1, m_2, m_3, m_4$  can be found numerically<sup>4</sup>. In particular, each fraction will have one limit (as  $t$  goes to 0 or 1)  $-\infty$  and the other limit  $1 - \delta$ , which means its supremum is either  $1 - \delta$ , or the value at one of its local maxima, whichever is greater.

## 4 Experiments

### 4.1 Setup

We implemented the parametric version of Epsilon\* and evaluated its values on two types of ML deep neural net (DNN) models trained on public data sets: UCI Adult<sup>5</sup> and Purchase-100<sup>6</sup>. The UCI Adult data set has about 48,000 data points and predicts the likelihood of someone having an income above \$50,000 based on demographic features obtained from the US census

<sup>4</sup>We observed in our implementation that for small values of  $\delta$ , the maximum of an  $m_i$  for  $i = 1, \dots, 4$  can occur at  $t$  very close to 0 or very close 1, which can lead to floating point errors. In our implementation, we avoid these errors by considering FNR and FPR values between  $(\delta, 1 - \delta)$ . Another approach to avoiding such numerical errors could be to consider Taylor-like approximations for the fractions in (11).

<sup>5</sup><http://archive.ics.uci.edu/ml>

<sup>6</sup><https://www.kaggle.com/c/acquire-valued-shoppers-challenge/data>



such as age and salary. We build a model to train on this data set following previously reported benchmark DNN architectures [Shokri et al.(2017)].

The Purchase-100 dataset consists of roughly 600 binary features and 300,000 records, with a multi-class vector output of dimension 100. We created an overly overfitted DNN model with three layers, each of 100 nodes, trained until the training accuracy was 100%. Over-fitting has been associated with poor privacy [Yeom et al.(2018)], as it results in a training output distribution that is different from the non-training output distribution.

#### 4.1.1 Privacy strategies

We considered several baseline models corresponding to training for different number of epochs (1, 5, 10, 20 epochs for Adult, and 10, 50, 100 for Purchase-100), as well as training with DP-SGD until reaching a DP  $\epsilon$  value of 1, 3, 10 and 100, where  $\delta$  was set to  $1/n \log n$ , for  $n$  = training set size. As showcased by other work [Denison et al.(2022), Ponomareva et al.(2023)], achieving good model utility when training with DP-SGD is non-trivial, and requires at the minimum a search through several hyperparameter values such as batch size, learning rate, clipping norm, and number of microbatches. We grid searched through a few hyper-parameter values inspired by recent work describing hyper-parameter tuning for DP-SGD [Denison et al.(2022)]: we used a SGD optimizer with a momentum value of 0.9 and learning rate of 0.01, and varied the clipping norm in the set {1, 10, 30}, the batch size in the set {64, 512} for Adult and {256, 1024} for Purchase-100, and the number of micro-batches in the set {1, 32}. We reached a desired DP epsilon value by performing a binary search on the noise multiplier parameter when all other parameter were set. This resulted in 51 experiments (hyper-parameter – privacy strategy combinations) for Purchase-100 and 52 experiments for Adult.

In performing the experiments, we fixed the training and non-training data sets (i.e. we do not resample), and repeated the experiments for each strategy five times to observe variability due to training with SGD. Note that, in plotting the privacy-utility landscape, we consider the DP parameter  $\epsilon$  used in training as part of the hyper-parameter set defining a *privacy mitigation* strategy, along with the other hyper-parameters (batch size, clip norm, etc.). In contrast, Epsilon\* describes a *measurement* for that strategy’s privacy risk. We measure the strategy’s utility using area under the receiver operating characteristic (AUROC) curve on the test set for the Adult models, and accuracy on the test set for Purchase-100 due to the multi-class objective. For training with DP, we used the TensorFlow Privacy library<sup>7</sup> (v.0.5.1), which utilizes a Rényi differential privacy (RDP)[Mironov(2017)] accountant function in order to estimate the DP parameter  $\epsilon$  used when training.

## 4.2 Results

To understand the privacy-utility trade-offs, we adopt a multi-objective decision-making framework [Rojers and Whiteson(2017)] where we show a privacy-utility plot for each data set and highlight the Pareto frontier on each plot. The Pareto frontier of a given set of points in the privacy-utility plane is the convex hull of strategies in this plane, taken in a direction that improves the privacy or the utility, i.e., any strategy on the Pareto frontier has the property that there are no two other strategies whose convex combination results in a point with higher utility or higher privacy.

We display values of utility and Epsilon\* for the public data set models. For each privacy-utility plot, in addition to highlighting the Pareto frontier, we also show marginal densities (using kernel density estimation) of the categories of strategies of the same type, e.g., marginal density of Epsilon\* for strategies where we train with DP versus baseline strategies where we do not, in order to visualize the relative values of the metrics for each category of strategies.

<sup>7</sup>[https://www.tensorflow.org/responsible\\_ai/privacy/guide](https://www.tensorflow.org/responsible_ai/privacy/guide)

### 4.2.1 Purchase-100

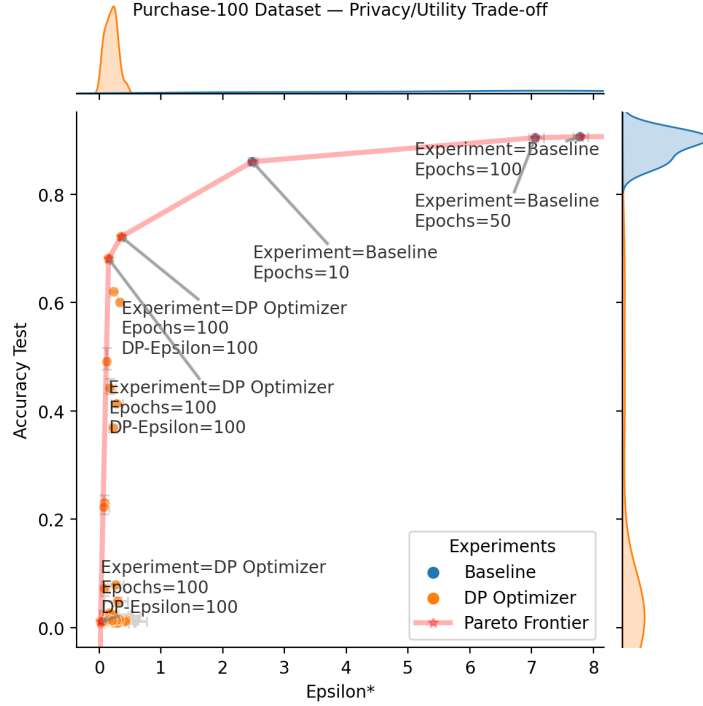


Figure 1: Privacy-Utility trade-off for the Purchase-100 model. Each point corresponds to one strategy (same hyperparameter set and privacy mitigation), averaged over five model instances. Error bars correspond to the minimum and maximum values over the five model instances.

Figure 1 displays the privacy-utility plot for the Purchase-100 data set. Each point is the average of five experiments with the same hyper-parameters and DP training  $\epsilon$  (if applicable), and therefore even if we trained to the same DP  $\epsilon$ , we may still have different utility and Epsilon\* values depending on the set of hyper-parameters used. For instance, we observe on the Pareto Frontier of Figure 1 multiple strategies trained with DP to the same  $\epsilon$  (in this case 100), but different hyper-parameter sets. Notice that, even though the Epsilon\* values for these three sets of experiments are relatively similar (and all less than 1), the test accuracy values are significantly different, varying from 1% to 72%. Similarly, we have multiple points for baseline models, corresponding to training for different number of epochs.

Baseline experiments that only vary the number of training epochs show that overfitting is correlated with poor privacy metrics, and provide a quantifiable value for the privacy-utility trade-off. We observe that increasing the number of training epochs increases the test accuracy of the model: 86% test accuracy when training for 10 epochs, to 90.4% when we train for 50, and 90.6% when we train for 100 epochs, but also increases Epsilon\* from 2.48 at 10 epochs to 7.06 at 50 epochs, and then 7.79 at 100 epochs. This behavior is consistent with the intuition that the more epochs we train, the more the model overfits, which results in higher privacy risk metric values.

When training with DP, Epsilon\* values become significantly smaller: the highest Epsilon\* experiments reach values of 7.8 for baseline models tuned with different hyperparameters, while all experiments where we train with DP had an Epsilon\* value below 1. This is also visible from the marginal density of Epsilon\* on the top of Figure 1, which is concentrated around values closer to 0 than to 1. However, DP has a sizable impact on model utility, as the marginal densities of accuracy values with and without DP, displayed on the right of the plot, also show. This is an example of the complexities of using DP in real-world scenarios that are commonly

discussed in the literature as well (e.g. Fig. 2, Section 5.4 in [Ponomareva et al.(2023)]), .

#### 4.2.2 Adult

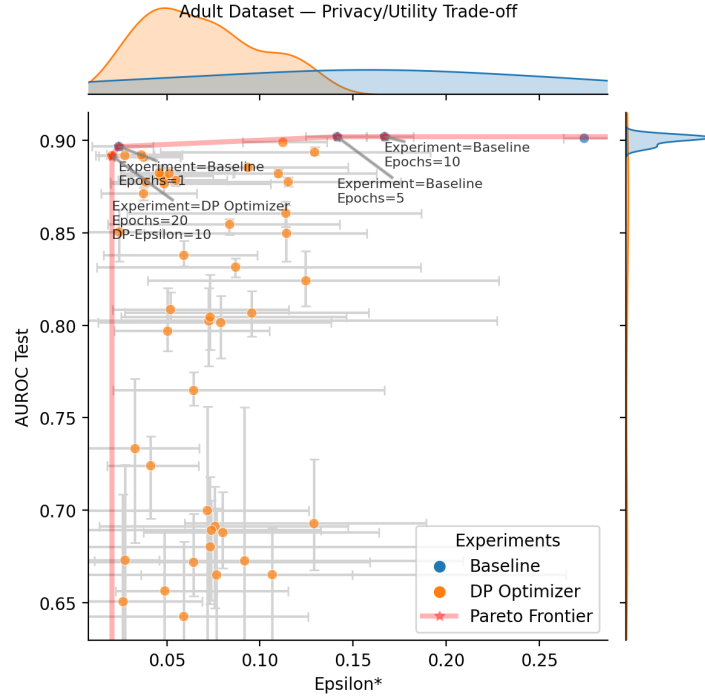


Figure 2: Privacy-Utility trade-off for the Adult model. Each point corresponds to one strategy (same hyperparameter set and privacy mitigation), averaged over five model instances. Error bars correspond to the minimum and maximum values over the five model instances.

Figure 2 shows the privacy-utility landscape for the Adult data set. We note that all our model instances resulted in  $\text{Epsilon}^*$  values below 0.3, which in comparison to Purchase-100, do not indicate privacy risk for this model across experiments and hyper-parameters. Even so, the model shows an increase in privacy risk as the number of epochs is increased for the baseline experiments. The “elbow” model instance in this Pareto frontier corresponds to a baseline model trained for a single epoch, which nonetheless outperforms most DP models as they lay below the Pareto frontier. We also note that even though the min-max ranges of  $\text{Epsilon}^*$  for the Adult experiments (error bars in Figure 2) appear to be larger than those for the Purchase-100 experiments, the absolute values of the averages are much smaller for Adult (less than 0.3) than for Purchase-100 (up to 7.8), indicating that the latter models likely exhibit generally higher privacy risk than the former.

## 5 Conclusion

We introduced  $\text{Epsilon}^*$ , a new privacy metric for measuring the privacy of a single model instance that enables privacy auditors to be independent of model owners: it does not require access to the data sampling pipeline or model training algorithm. We show how  $\text{Epsilon}^*$  can be derived from a model-level  $(\epsilon, \delta)$  quantification of privacy to which the hypothesis test formulation of DP can be extended. We established a relationship between  $\text{Epsilon}^*$  and a lower bound on the privacy loss of the training mechanism, and show how to implement  $\text{Epsilon}^*$  to avoid numerical and noise amplification instability. We further show in experiments on benchmark

public data sets that Epsilon\* is sensitive to privacy mitigation with DP, and therefore can stand as a reliable privacy metric for machine learning models.

## 6 Acknowledgments

The authors would like to thank Ryan Rogers, Rina Friedberg and Mark Yang for their constructive peer feedback that greatly improved the clarity of this manuscript.

## References

- [Andrew et al.(2023)] Galen Andrew, Peter Kairouz, Sewoong Oh, Alina Oprea, H Brendan McMahan, and Vinith Suriyakumar. 2023. One-shot Empirical Privacy Estimation for Federated Learning. *arXiv preprint arXiv:2302.03098* (2023).
- [Bichsel et al.(2018)] Benjamin Bichsel, Timon Gehr, Dana Drachler-Cohen, Petar Tsankov, and Martin Vechev. 2018. DP-finder: Finding differential privacy violations by sampling and optimization. In *Proceedings of the 2018 ACM SIGSAC Conference on Computer and Communications Security*. 508–524.
- [Carlini et al.(2022)] Nicholas Carlini, Steve Chien, Milad Nasr, Shuang Song, Andreas Terzis, and Florian Tramèr. 2022. Membership Inference Attacks From First Principles. In *2022 IEEE Symposium on Security and Privacy (SP)*. 1897–1914.
- [Denison et al.(2022)] Carson Denison, Badih Ghazi, Pritish Kamath, Ravi Kumar, Pasin Manurangsi, Krishna Giri Narra, Amer Sinha, Avinash Varadarajan, and Chiyuan Zhang. 2022. Private Ad Modeling with DP-SGD. *arXiv preprint arXiv:2211.11896* (2022).
- [Ding et al.(2018)] Zeyu Ding, Yuxin Wang, Guanhong Wang, Danfeng Zhang, and Daniel Kifer. 2018. Detecting violations of differential privacy. In *Proceedings of the 2018 ACM SIGSAC Conference on Computer and Communications Security*. 475–489.
- [Dong et al.(2022)] Jinshuo Dong, Aaron Roth, and Weijie J Su. 2022. Gaussian differential privacy. *Journal of the Royal Statistical Society Series B: Statistical Methodology* 84, 1 (2022), 3–37.
- [Dwork et al.(2006)] Cynthia Dwork, Frank McSherry, Kobbi Nissim, and Adam Smith. 2006. Calibrating noise to sensitivity in private data analysis. In *Theory of Cryptography: Third Theory of Cryptography Conference, TCC 2006, New York, NY, USA, March 4–7, 2006. Proceedings 3*. Springer, 265–284.
- [Jagielski et al.(2020)] Matthew Jagielski, Jonathan Ullman, and Alina Oprea. 2020. Auditing Differentially Private Machine Learning: How Private is Private SGD?. In *Advances in Neural Information Processing Systems*, H. Larochelle, M. Ranzato, R. Hadsell, M.F. Balcan, and H. Lin (Eds.), Vol. 33. Curran Associates, Inc., 22205–22216.
- [Jayaraman et al.(2020)] Bargav Jayaraman, Lingxiao Wang, Katherine Knipmeyer, Quanquan Gu, and David Evans. 2020. Revisiting membership inference under realistic assumptions. *arXiv preprint arXiv:2005.10881* (2020).
- [Kairouz et al.(2015)] Peter Kairouz, Sewoong Oh, and Pramod Viswanath. 2015. The composition theorem for differential privacy. In *International conference on machine learning*. PMLR, 1376–1385.

- [Lu et al.(2022)] Fred Lu, Joseph Munoz, Maya Fuchs, Tyler LeBlond, Elliott Zaresky-Williams, Edward Raff, Francis Ferraro, and Brian Testa. 2022. A General Framework for Auditing Differentially Private Machine Learning. *arXiv preprint arXiv:2210.08643* (2022).
- [Maddock et al.(2022)] Samuel Maddock, Alexandre Sablayrolles, and Pierre Stock. 2022. CAN-IFE: Crafting Canaries for Empirical Privacy Measurement in Federated Learning. *arXiv preprint arXiv:2210.02912* (2022).
- [Mironov(2017)] Ilya Mironov. 2017. Rényi differential privacy. In *2017 IEEE 30th computer security foundations symposium (CSF)*. IEEE, 263–275.
- [Nasr et al.(2023)] Milad Nasr, Jamie Hayes, Thomas Steinke, Borja Balle, Florian Tramèr, Matthew Jagielski, Nicholas Carlini, and Andreas Terzis. 2023. Tight Auditing of Differentially Private Machine Learning. *arXiv preprint arXiv:2302.07956* (2023).
- [Nasr et al.(2021)] Milad Nasr, Shuang Songi, Abhradeep Thakurta, Nicolas Papernot, and Nicholas Carlin. 2021. Adversary Instantiation: Lower Bounds for Differentially Private Machine Learning. In *2021 IEEE Symposium on Security and Privacy (SP)*. 866–882.
- [Ponomareva et al.(2023)] Natalia Ponomareva, Hussein Hazimeh, Alex Kurakin, Zheng Xu, Carson Denison, H Brendan McMahan, Sergei Vassilvitskii, Steve Chien, and Abhradeep Thakurta. 2023. How to dp-fy ml: A practical guide to machine learning with differential privacy. *arXiv preprint arXiv:2303.00654* (2023).
- [Rojers and Whiteson(2017)] Diederik M Roijers and Shimon Whiteson. 2017. Multi-objective decision making. *Synthesis lectures on artificial intelligence and machine learning* 11, 1 (2017), 1–129.
- [Salem et al.(2018)] Ahmed Salem, Yang Zhang, Mathias Humbert, Pascal Berrang, Mario Fritz, and Michael Backes. 2018. ML-leaks: Model and data independent membership inference attacks and defenses on machine learning models. *arXiv preprint arXiv:1806.01246* (2018).
- [Shokri et al.(2017)] Reza Shokri, Marco Stronati, Congzheng Song, and Vitaly Shmatikov. 2017. Membership inference attacks against machine learning models. In *2017 IEEE symposium on security and privacy (SP)*. IEEE, 3–18.
- [Steinke et al.(2023)] Thomas Steinke, Milad Nasr, and Matthew Jagielski. 2023. Privacy Auditing with One (1) Training Run. *arXiv preprint arXiv:2305.08846* (2023).
- [Tramer et al.(2022)] Florian Tramer, Andreas Terzis, Thomas Steinke, Shuang Song, Matthew Jagielski, and Nicholas Carlini. 2022. Debugging differential privacy: A case study for privacy auditing. *arXiv preprint arXiv:2202.12219* (2022).
- [Ye et al.(2022)] Jiayuan Ye, Aadyaa Maddi, Sasi Kumar Murakonda, Vincent Bindschaedler, and Reza Shokri. 2022. Enhanced membership inference attacks against machine learning models. In *Proceedings of the 2022 ACM SIGSAC Conference on Computer and Communications Security*. 3093–3106.
- [Yeom et al.(2018)] Samuel Yeom, Irene Giacomelli, Matt Fredrikson, and Somesh Jha. 2018. Privacy Risk in Machine Learning: Analyzing the Connection to Overfitting. In *2018 IEEE 31st Computer Security Foundations Symposium (CSF)*. 268–282.
- [Zanella-Béguelin et al.(2022)] Santiago Zanella-Béguelin, Lukas Wutschitz, Shruti Tople, Ahmed Salem, Victor Rühle, Andrew Paverd, Mohammad Naseri, and Boris Köpf. 2022. Bayesian estimation of differential privacy. *arXiv preprint arXiv:2206.05199* (2022).

## 7 Appendix A: Proofs

### 7.1 Proof of Theorem 3

*Proof.* If mechanism  $M$  is  $(\epsilon, \delta)$ -DP, per (1), then if we fix  $(x, y) \in \mathcal{X} \times \mathcal{Y}$ , we must have that for any two neighboring data sets  $D$  and  $D'$

$$\mathbb{P}_{\theta \sim M(D)} [(f_\theta(x), y) \in R_\theta] \leq e^\epsilon \mathbb{P}_{\theta \sim M(D')} [(f_\theta(x), y) \in R_\theta] + \delta, \quad (22)$$

where on the left side the probability is with respect to the randomness of the training mechanism using  $D$  as training set, and on the right using  $D'$ . Note that (22) holds regardless of the choice of the set  $R_\theta$ , assuming a measurability of the mapping  $\theta \rightarrow R_\theta$ . (22) also holds whether or not  $(x, y)$  is in  $D$  and/or  $D'$ .

If  $D = \{(x_1, y_1), \dots, (x_n, y_n)\}$ , then for each  $i = 1, \dots, n$  we can use (22) for the pair  $(x_i, y_i)$  and any set  $D'_i = D \setminus (x_i, y_i)$ . Summing up the resulting inequality over all points in  $D$  and averaging, gives us

$$\frac{1}{n} \sum_{i=1}^n \mathbb{P}_{\theta \sim M(D)} [(f_\theta(x_i), y_i) \in R_\theta] \leq e^\epsilon \frac{1}{n} \sum_{i=1}^n \mathbb{P}_{\theta \sim M(D'_i)} [(f_\theta(x_i), y_i) \in R_\theta] + \delta \quad (23)$$

We can now take expectation in (23) over all training sets  $D$ . The left side of (23) averages to the left side of (13), with different notation. The right side of (23) averages to the right side of (13), with the difference that the training set over which the expectation is taken is of size  $n - 1$  instead of  $n$ . However, for large  $n$ , this difference becomes negligible, and we obtain (13)

$$E_{D, \theta} [\mathbb{P}_{(X, Y) \sim D} [(f_\theta(X), Y) \in R_\theta]] \leq e^\epsilon E_{D, \theta} [\mathbb{P}_{(X, Y) \sim \bar{D}} [(f_\theta(X), Y) \in R_\theta]] + \delta.$$

(12) can be obtained analogously by switching  $D$  with  $D'$  in (22). This implies that any  $\epsilon$  that breaks either (12) or (13) cannot satisfy the DP property (22), so an  $\bar{\epsilon}$  that satisfies both is a lower bound for the  $\epsilon$  of  $M$ . □

### 7.2 Proof of Theorem 4

We want to prove that

$$\bar{\epsilon} \leq \log \left[ E_\theta \left( e^{\epsilon^*} \right) \right],$$

where  $\bar{\epsilon}$  be the mechanism-level lower bound on privacy loss as in (15):

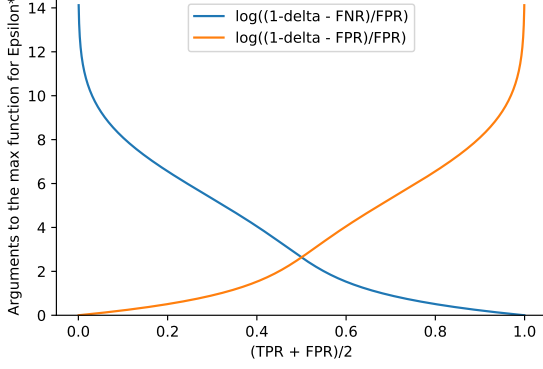
$$\bar{\epsilon} = \log \left[ \max_{i=1, \dots, k} \max \left( \frac{1 - \delta - \eta_{t_i}}{t_i}, \frac{1 - \delta - t_i}{\eta_{t_i}}, \frac{\eta_{t_i} - \delta}{1 - t_i}, \frac{t_i - \delta}{1 - \eta_{t_i}} \right) \right],$$

and  $\epsilon^* = \epsilon^*(\theta)$  is the (random) individual model-level lower bound on privacy loss as in (16):

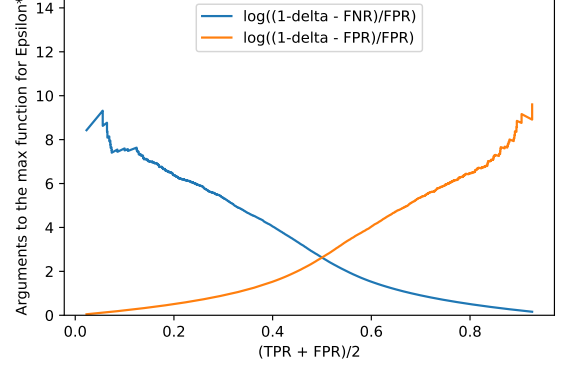
$$\epsilon^* = \epsilon^*(\theta) = \log \left[ \max_{i=1, \dots, k} \max \left( \frac{1 - \delta - \eta_{t_i}(\theta)}{t_i}, \frac{1 - \delta - t_i}{\eta_{t_i}(\theta)}, \frac{\eta_{t_i}(\theta) - \delta}{1 - t_i}, \frac{t_i - \delta}{1 - \eta_{t_i}(\theta)} \right) \right].$$

*Proof.* Notice that for each  $t > 0$ , the functions  $\frac{1 - \delta - \eta}{t}$ ,  $\frac{(1 - \delta - t)_+}{\eta}$ ,  $\frac{\eta - \delta}{1 - t}$ ,  $\frac{(t - \delta)_+}{1 - \eta}$  are all convex functions of  $0 < \eta < 1$ . Furthermore, the maximum of convex functions is itself a convex function. Therefore,

$$\max_{i=1, \dots, k} \max \left( \frac{1 - \delta - \eta_{t_i}(\theta)}{t_i}, \frac{1 - \delta - t_i}{\eta_{t_i}(\theta)}, \frac{\eta_{t_i}(\theta) - \delta}{1 - t_i}, \frac{t_i - \delta}{1 - \eta_{t_i}(\theta)} \right)$$



(a) Evaluating the CDFs of the true loss distributions



(b) Evaluating the empirical CDFs from samples of the loss distributions

Figure 3: First two expressions in (11), when evaluating the true versus the empirical CDFs from sampled data

is a convex function of the random vector  $(\eta_{t_i}(\theta), i = 1, \dots, k)$ . Taking expectation with respect to the randomness of the model weights  $\theta$  gives us, by Jensen's inequality,

$$\begin{aligned} E\left(e^{\epsilon^*(\theta)}\right) &= E\left[\max_{i=1,\dots,k} \max\left(\frac{1-\delta-\eta_{t_i}(\theta)}{t_i}, \frac{1-\delta-t_i}{\eta_{t_i}(\theta)}, \frac{\eta_{t_i}(\theta)-\delta}{1-t_i}, \frac{t_i-\delta}{1-\eta_{t_i}(\theta)}\right)\right] \\ &\geq \max_{i=1,\dots,k} \max\left(\frac{1-\delta-E[\eta_{t_i}(\theta)]}{t_i}, \frac{1-\delta-t_i}{E[\eta_{t_i}(\theta)]}, \frac{E[\eta_{t_i}(\theta)]-\delta}{1-t_i}, \frac{t_i-\delta}{1-E[\eta_{t_i}(\theta)]}\right) \\ &= e^{\bar{\epsilon}} \end{aligned}$$

where we used (14). We conclude that

$$\bar{\epsilon} \leq \log\left[E_{\theta}\left(e^{\epsilon^*}\right)\right]$$

□

## 8 Appendix B: Parametric vs Empirical Epsilon\*

Recall from Equation (11) that Epsilon\* is computed from the estimated FNRs  $\eta_i$  and FPRs  $t_i$  of the hypothesis test of the MIA adversary.

$$\epsilon^* = \log\left[\max_{i=1,\dots,k} \max\left(\frac{1-\delta-\eta_i}{t_i}, \frac{1-\delta-t_i}{\eta_i}, \frac{\eta_i-\delta}{1-t_i}, \frac{t_i-\delta}{1-\eta_i}\right)\right]$$

Accurate estimates of FNRs and FPRs are therefore crucial to the accuracy of Epsilon\*. In fact, the main cause for inaccurate values of Epsilon\* is noise amplification when the TPR/FPR becomes close to 0 and 1, which can be additionally inflated by numerical instability from computation involving maxima over logs of (ratios of) very small numbers.

To better visualize the noise impact, Figure 3 shows the values of the first two quantities in (11) versus  $\frac{1}{2}(TPR + FPR)$  when we simulate loss data from known Gaussian distributions ( $\mathcal{N}(0,1)$  for training and  $\mathcal{N}(3,1)$  for non-training) and compute the FNR's and FPRs either by directly evaluating the CDFs of the known loss distributions (a), or by evaluating the empirical CDFs of simulated losses (b). In both cases, we remove FNR and FPR values less than  $10^{-9}$  for numerical stability. As seen in Figure 3, most noise and most signal occurs at the very ends of the FNR/ FPR arrays, since Epsilon\* is the maximum over (noisy) quantities in 11, and that maximum occurs in the noisiest part of the curves.

## 8.1 Simulation of Empirical vs Parametric Epsilon\*

To evaluate the impact of noise amplification and mitigation strategies, we set up a simulation where we decide what the true loss distributions are, and generate loss samples from these distributions. This allows us to compare the Epsilon\* values from evaluating the true TPR/FPRs CDFs versus estimating TPR/FPR values from sampled losses empirically.

In our simulation, we mostly focus on Gamma loss distributions, as they have the desired support in  $[0, \infty)$ . Specifically, we consider the training and non-training set losses to be Gamma distributed with parameters  $(k_1, \theta_1)$  and  $(k_2, \theta_2)$  respectively. Our goal for this simulation is to compare the values of Epsilon\* when the *FNRs* and *FPRs* used to compute it in Equation (11) are obtained by either:

- directly evaluating the CDFs of the known Gamma distributions used to generate the training and non-training losses;
- evaluating the empirical CDFs of the sampled training and non-training losses; or
- fitting Normal distributions to a transformation of the losses, then evaluating the CDFs of the fitted parametric distributions.

The transformation of losses mentioned in the last bullet point is the following, similar to the one used by [Carlini et al. (2022)]:

1. Normalize losses to  $[0,1]$  by subtracting  $\min(\text{train loss}, \text{non-train loss})$  from each loss value and dividing by  $(\max(\text{train loss}, \text{non-train loss}) - \min(\text{train loss}, \text{non-train loss}))$ .
2. Shift the normalized losses from step 1 away from 0 by adding  $\alpha$  ( $=1$ ).
3. Exponentiate the negative of losses in step 2:  $p = \exp(-\text{Step 2 losses})$ .
4. Pass the losses from Step 3 through a logit function:  $\phi = \log(p) - \log(1 - p)$

Note that the first option is only available in our simulation, as in practice we do not possess knowledge of the true distributions generating the observed losses. In each of the three variants, we evaluate the CDFs at 2 million points corresponding to 1 million equally spaced quantiles of the training distribution and 1 million equally spaced quantiles of the non-training distribution. For numerical stability, we remove FNR and FPR values outside the interval  $(0.001, 0.999)$  for the empirical Epsilon\* and outside the interval  $(\delta, 1 - \delta)$  for the parametric Epsilon\*.

We also inspect the impact of loss set sample size  $n$  by varying it in the set  $\{10^3, 10^4, 10^5\}$ . To evaluate the noise in our Epsilon\* values, we repeat the sampling (of size  $n$ ) and computation of Epsilon\* values  $k$  times, where  $k = 10$ .

We investigate the relative values of the three Epsilon\* implementation in two regimes: when the true training and non-training loss distributions are identical, implying that Epsilon\* should have a value of 0; and when the true loss distributions are farther and farther apart. We simulate the latter case by considering the true training loss distribution to be  $\Gamma(k_1, \theta_1)$ , and the true non-training loss distribution to be  $\Gamma(k_1 + d, \theta_1)$ , for  $d \in \{1, 2, 3\}$ ,  $k_1 = 2$ ,  $\theta_1 = 5$ .

### 8.1.1 Identical Loss Distributions

A special case worth examining in our simulation is when the true training and non-training loss distributions are identical. This means that the true Epsilon\* is 0, and therefore implementations that get closer to that value are more accurate. However, neither the empirical nor parametric implementations have visibility into the true loss distributions, as they only observe the set of losses sampled from those distributions.

We show the values of Epsilon\* (means and standard deviations over the 10 runs) computed with the empirical and the parametric fits to the loss distributions in Figure 4. We make two



observations based on this figure: 1) The parametric implementations shows values closer to the true value of 0 than the empirical implementation; and 2) there is an impact of the loss sample size: the larger the loss sample size, the closer both implementations get to the true value of 0.

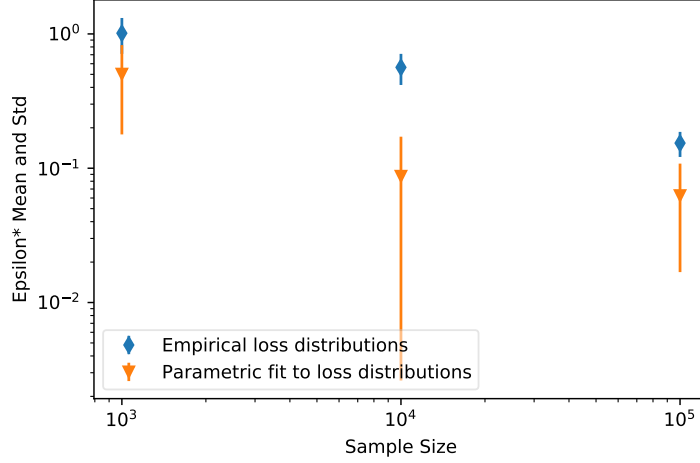


Figure 4: Epsilon\* from empirical vs parametric fitted distributions to loss data when the true training and non-training distributions are identical

### 8.1.2 Increasing the distance between training and non-training distributions

We now explore in simulation what happens when the training and non-training loss distributions are farther and farther apart. We simulate this by increasing the parameter  $d$ , where the true training and non-training distributions are  $\Gamma(k_1, \theta_1)$ , and  $\Gamma(k_1 + d, \theta_1)$  respectively, for  $d \in \{0, 1, 2, 3\}$ . Since Figure 4 showed that the sample size can influence the accuracy of Epsilon\*, we also vary the training and non-training sample size  $n$  in the set  $\{10^3, 10^4, 10^5\}$ .

The mean and standard deviation of the Epsilon\* values over 10 runs of the simulation are shown in Figure 5. This Figure confirms the findings of Figure 4 when  $d = 0$ , meaning that the empirical implementation overshoots the true value of 0 when  $d = 0$  more than the parametric implementation, but also shows that the empirical implementation values undershoot the true Epsilon\* values more than those of the parametric implementation as the distance  $d$  between training and non-training loss distributions increases. Just as in Figure 4, this bias is exacerbated for smaller sample sizes but can be mitigated by increasing loss set sample sizes. We conclude from this simulation that fitting parametric distributions to loss data in order to estimate the FNRs and FPRs used in the Epsilon\* computation leads to more accurate values than using empirical CDFs of the loss distributions.

## 8.2 Goodness-of-fit for Parametric Distributions Fitted to Loss Data

As described in Section 8.1, we fit Normal distributions to the transformed train and non-train losses in order to estimate the FNRs and FPRs required by the evaluation of Epsilon\*. In order to evaluate the quality of the parametric fitting, we perform 2-sample Kolmogorov-Smirnov (KS) goodness-of-fit statistical tests which measure the maximum distance between the empirical CDFs of the two samples and tests the hypothesis that the underlying distributions are identical.

We evaluate the goodness-of-fit test not only for a Normal distribution, but for more general Gaussian Mixture Models (GMMs) with up to 20 components. To perform the KS test, we:

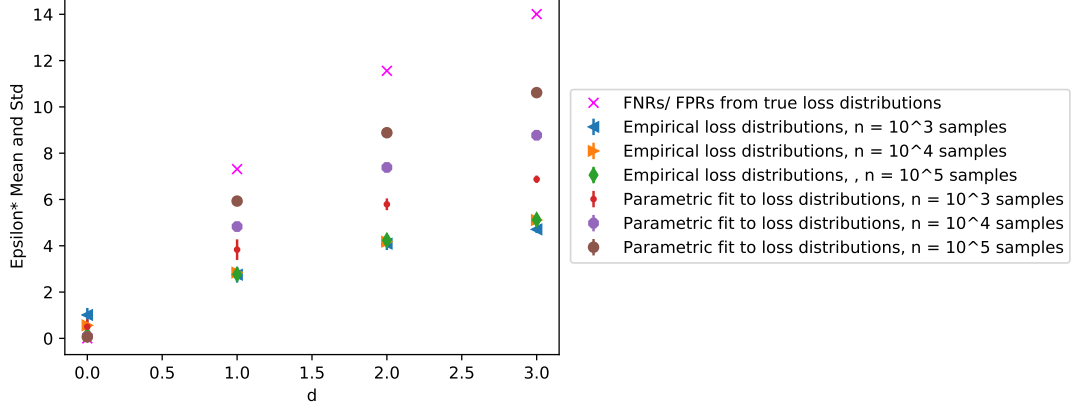


Figure 5: Epsilon\* from empirical vs parametric fitted distributions to loss data when the true training and non-training distributions are  $\Gamma(k_1, \theta_1)$ , and  $\Gamma(k_1 + d, \theta_1)$  respectively, for  $d \in \{0, 1, 2, 3\}$ ,  $k_1 = 2$ ,  $\theta_1 = 5$ .

1. Partition the given loss set (be it training or non-training) into a fitting set and an evaluation set, where the latter has size  $n_{samples}$ .
2. Fit a GMM with  $n_{components}$  to the fitting set from Step 1.
3. Sample a set of  $n_{samples}$  from the GMM fitted in Step 2.
4. Perform a 2-sample Kolmogorov-Smirnov (KS) test comparing the evaluation set to the set of samples generated by the GMM.

We vary  $n_{components}$  from 1 to 20, and  $n_{samples}$  from 100 to 1,000.

We are particularly interested in whether the p-value of the KS test goes above  $\alpha = 0.05$  for any fitted GMM model, as that indicates that the null hypothesis (that the underlying distributions are identical) cannot be rejected at that confidence level.

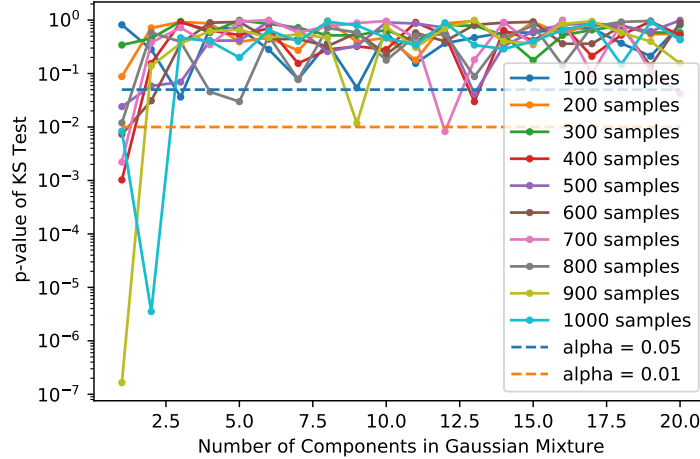


Figure 6: p-values from KS tests of goodness-of-fit for a model instance of the baseline Adult data set.

Figure 6 shows the p-value of the KS test comparing GMMs of increasing number of components to a sample of the transformed training losses for an instance of the Adult model trained without DP. We find that most p-values go above 0.05, especially as the number of components in the GMM is increased. For most sample sizes ( $n_{samples}$ ), even only one component in the

GMM results in p-values above 0.05, therefore, in order to keep the complexity of the fitted distribution as low as possible, we decided to keep the one-component (Normal distribution) in our implementation.